Title: Impact of Hydrodynamics on iPSC-derived Cardiomyocyte Differentiation Processes

Authors: Jasmin J Samaras[a], Bernardo Abecasis[b,c], Margarida Serra[b,c], Andrea Ducci[d], Martina Micheletti[a]

Affiliations: [a] Advanced Centre for Biochemical Engineering, University College London, Bernard Katz Building, Gower Street, London, WC1E 6BT, United Kingdom

jasmin.samaras.10@ucl.ac.uk , m.micheletti@ucl.ac.uk

[b] iBET, Instituto de Biologia Experimental e Tecnológica, Av. República, Qta. do Marquês, Estação Agronómica Nacional, Edificio IBET/ITQB, Oeiras, Portugal

babecasis@itqb.unl.pt, mserra@itqb.unl.pt

[c] Instituto de Tecnologia Química e Biológica António Xavier, Universidade Nova de Lisboa, Av. da República, 2780-157 Oeiras, Portugal

[d] Department of Mechanical Engineering, University College London, Torrington Place,

London, WC1E 7JE, United Kingdom

a.ducci@ucl.ac.uk

Corresponding Author:

Dr Martina Micheletti,

Advanced Centre for Biochemical Engineering, University College London, Bernard Katz Building, Gower Street, London, WC1E 6BT, United Kingdom

+44 20 7679 9787 m.micheletti@ucl.ac.uk

Abstract

Cardiomyocytes (CMs), derived from pluripotent stem cells (PSCs), have the potential to be used in cardiac repair. Addition of physical cues, such as electrical and mechanical stimulations, have proven to significantly effect morphology, density, cardiogenesis, maturity and functionality of differentiated CMs. This work combines rigorous fluid dynamics investigation and flow frequency analysis with iPSC differentiation experiments to identify and quantify the flow characteristics leading to a significant increase of differentiation yield. This is towards a better understanding of the physical relationship between frequency modulation and embryoid bodies suspension, and the development of dimensionless correlations applicable at larger scales.

Laser Doppler Anemometry and Fast Fourier Transform analysis were used to identify characteristic flow frequencies under different agitation modes. Intermittent agitation resulted in a pattern of low intensity frequencies at reactor scale that could be controlled by varying three identified time components: rotational speed, interval and dwell times. A proof of concept biological study was undertaken, tuning the hydrodynamic environment through variation of dwell time based on the engineering study findings and a significant improvement in CM yield was obtained. This work introduces the concept of fine-tuning the physical hydrodynamic cues within a three-dimensional flow system to improve cardiomyocyte differentiation of iPSC.

Key words: Cardiomyocyte differentiation, hydrodynamics, FFT, suspension dynamics, induced pluripotent stem cells

[1]

[1] Abbreviations: CM, cardiomyocytes; EB, embryoid body; FDA, fluorescein diacetate; FFT, fast Fourier transform; hESC, human embryonic stem cells; iPSC, induced pluripotent stem cells; PI, propidium iodide; PSC, pluripotent stem cells

1. Introduction

Kehat *et al.* were the first to derive early-stage cardiomyocytes (CMs) from an embryoid body-based culture of human embryonic stem cells (hESCs) (Kehat et al., 2001). Since then, an increasing amount of research into regeneration of the human heart through implantation of stem cell-derived CMs has been undertaken. The clinical trial ESCORT (ClinicalTrials.gov identifier: NCT02057900; Phase I), investigating the transplantation of cardiac progenitors derived from hESC embedded in a fibrin scaffold, is currently ongoing (Menasche et al., 2015). Applications of pluripotent stem cell (PSC)-derived CMs such as drug screening, cardiotoxicity and disease modelling are also being explored.

To ascertain effective differentiation strategies, understanding how cardiac lineage is established from an early embryo is fundamental and many studies have investigated recapitulation of cardiogenesis *in vitro* to improve efficiency and yield. Ge *et al*. proved that bone marrow-mesenchymal stem cells were capable of differentiating into CMs when cultivated in monolayers using 4 % cyclic strain at 1 Hz (Ge et al., 2009). Lam *et al*. compared ESC monolayer cultures, microcarrier-based static and shaken suspensions with stirred spinner flask and reported a 10-fold higher cardiogenic differentiation yield in intermittently stirred conditions. In this case, two 16 hour dwell phases were introduced at day 0 and on day 3 of culture (Lam et al., 2014). Ting *et al*. found improved cardiomyogenesis can be obtained when agitation is applied intermittently to ESC-seeded microcarrier cultures using a rocker platform. The application of intermittent agitation for the first 3 days of differentiation was applied with 6 minutes of motion followed by a static 66 minutes dwell phase. This increased differentiation yields by 40 % in comparison with static cultures (Ting et al., 2014). Due to the excessive dwell phases applied in both studies, the observed biological outcomes are no longer related to flow cues, but are likely to be as a result of introducing intermittent monolayer culture conditions.

Correia *et al.* developed a robust and scalable platform for iPSC-CM differentiation, combining a three-dimensional agitation profile strategy with hypoxic conditions. Three different impeller agitation profiles were used to subject iPSCs to a range of flow configurations: continuous, intermittent with and without a direction change in impeller rotation. An overall 1000-fold improvement in CM yield was achieved using intermittent agitation and hypoxic conditions in comparison to normoxic continuously agitated cultures (Correia et al., 2014). Several studies have investigated the optimal conditions to reproducibly generate high numbers of CMs using various protocols, however, few publications have considered engineering aspects such as the quality of suspension and the impact of characteristic flow frequencies (*f*) upon differentiation. A number of studies have explored the application of frequencies in the range of 0.033 to 1 Hz, induced from hydrodynamic interactions or stretch/strain devices, resulting in varying degrees of improvement to cardiomyogenesis when compared to use of biochemical cues alone (Correia et al., 2014; Geuss and Suggs, 2013; Ting et al., 2014).

Cell culture studies often focus on biological parameters without suspension characterization of a bioreactor. The quality of embryoid bodies (EBs) suspension is important to prevent EB agglomeration and ensure uniform exposure to characteristic flow frequencies, as well as avoidance of spatial pH, oxygen and nutrient gradients (Lara et al., 2006). Inhomogeneity in the cell culture may also result in a more pronounced mixed population of differentiated cells. Suspension of EBs is primarily affected by the selected rotational speed, however, the use of different agitation modes during cell culture may result in a degree of EB settling during the intermittent intervals. In addition, the degree of settling depends on the EB size, morphology and density, properties which are likely to change over the course of cell culture. Suspension should therefore be characterized to quantify the minimum speed required for off-bottom suspension and homogeneity, but also to characterize the degree of settling during

intermittent agitation modes. Off-bottom suspension has been studied in-depth (Ibrahim and Nienow, 2004; Nienow et al., 2016), however objective techniques and reproducible protocols should be used to quantify suspension (Olmos et al., 2015; Pieralisi et al., 2016).

In this 'proof of concept' work an in-depth investigation of flow frequency and suspension characteristics under different agitation modes is presented. iPSC differentiation experiments were also conducted to demonstrate the impact of flow characteristics on cell phenotype, differentiation efficiency and yield.

2. Materials and Methods

2.1. Bioreactor Configuration

A flat-bottomed DASGIP Cellferm-Pro bioreactor system (Eppendorf, Germany), with height, H = 15.5 cm, and internal diameter, D_v = 6.2 cm, was equipped with a 6 cm diameter trapezoidal paddle impeller at an off-bottom clearance, C = 1.4 cm (D_i/D_v = 0.97, C/D_v = 0.2). A working volume of V_w= 200 mL was used, corresponding to a liquid height, H_L = 6.62 cm. For both the engineering characterization and cell culture experiments, modifications were made to the original magnetically-driven bioreactor to achieve motor-driven agitation. The impeller shaft was extended and attached to an N-Series Allen Bradley Motor unit. For the engineering characterization studies (described in Sections 2.2 and 2.3) the system was mounted within a water filled glass trough, shown in Figure 1, filled with water such as to minimize optical distortion due to the curvature of the vessel. iPSC culture experiments (described in Section 2.4) were performed using the DASGIP BioBlock, equipped with an on-line data acquisition and control DASware 4.0 software (Eppendorf, Germany).

2.2. Laser Doppler Anemometry and Data Processing

Measurements of the tangential and axial velocity components were carried out using a Laser Doppler Anemometry system. A Stellar Pro-L ML/300 Argon ion laser (Modu-Laser, USA)

was used for these experiments. Two pairs of intersecting laser beams were emitted at wavelengths of 514.5 nm and 488 nm, measuring velocities in the tangential and axial directions, respectively. The BSA Flow software (Dantec Dynamics A/S, Skovlunde, Denmark) was used for data recording. For these experiments MilliQ water was used, seeded with neutrally buoyant PSP-20 Polyamid 20 μm particles obtained from Dantec Dynamics (A/S, Skovlunde, Denmark). A cylindrical coordinate reference system (*r*, *θ*, *z)* was employed, as shown in Figure 1, with the origin positioned at the center of the base and the tangential coordinate, *θ*, increasing anti-clockwise when seen from above. Measurements were performed at two locations, location **A** close to the impeller (r/D_v = 0.5 and z/H = 0.18) and location **B** within the bulk flow (r/D_v = 0.5 and z/H = 0.24). Tangential velocities were converted into the frequency domain using a Fast Fourier Transform (FFT) approach. Continuous and intermittent agitation modes were investigated in this work. For intermittent agitation, three time components were defined, namely the impeller rotational speed *N*, the interval time T_{inv} and the dwell/stop time T_{dwell}. T_{inv} is the time during which the impeller is in motion and T_{dwell} defines how long the impeller is stopped. In Correia *et al.* (2014) *N* = 90 rpm was used and continuous and intermittent motion with and without a direction change were investigated at T_{inv} = 30 s and T_{dwell} = 900 ms. A parametric study investigating the effect of a change in T_{inv} and T_{dwell} was performed in this work. Three interval times were considered, T_{inv} = 5 s, 15 s and 30 s at constant T_{dwell} = 500 ms and *N* = 90 rpm. The dwell time was then also investigated within the range T_{dwell} = 1 ms – 1500 ms at constant T_{inv} = 30 s and *N* = 90 rpm. In addition, studies were carried out at different rotational speeds where the number of missed revolutions, *K***, defined by Equation (1), was kept constant:

$$K^{**} = N \times T_{dwell} \qquad (1)$$

At *N* = 90 rpm, T_{inv} = 30 s and T_{dwell} = 1500 ms a value of K^{**} = 2.25 was calculated and maintained constant in subsequent experiments conducted at *N* = 75, 105 and 120 rpm.

2.3. Suspension Characterization Experiments

Suspension characterization measurements were performed using a similar experimental set up to Figure 1, with a mounted high-speed NET iCube camera (NET, Germany) connected to an adjustable arm in place of the laser. The camera was fitted with a macro lens to capture small variations in image brightness and improve system resolution and was used to acquire sets of images at increasing speeds using different agitation strategies. A white LED panel was installed behind the reactor to minimize background noise. Continuous impeller agitation was used to investigate the minimum speed required to achieve homogeneity, N_H, for N = 10 – 200 rpm. Intermittent agitation conditions were investigated at N = 90 rpm, T_{inv} = 30 s and T_{dwell} = 500 - 30,000 ms to observe the impact upon suspension for increasing T_{dwell} until T_{dwell} = T_{inv} = 30 s. Two types of microcarriers, Cytodex 3 (ρ = 1.04 g/mL, average particle diameter D_{50} = 175 μm, GE Healthcare, USA) and Cultispher-G (ρ = 1.04 g/mL, D_{50} = 255 μm, Percell Biolytica, Sweden) were used in these experiments to mimic the EB suspension at the start (day 2) and at the end (day 9) of the differentiation process, respectively. They were selected based on the EB sedimentation characteristics and sizes (iBET group, unpublished data). Microcarriers were stained using 0.4 % Trypan Blue (Sigma-Aldrich, USA) to aid in visualization (Olmos et al., 2015), and experiments were conducted at a concentration of 1 g/L. Concentrations closer to those employed in cell culture experiments (0.0375 g/L at the start of differentiation and 0.2 g/L at the end) could not be detected by the camera. Images were recorded at a frequency of 2 Hz for 5 minutes per condition to ensure 'steady state' was captured during measurement. The microcarriers were then allowed to fully settle in-between experiments. Images were processed using a purposely-written MATLAB code where a suspension index, $S_{(N)}$, was determined with Equation (2):

$$S_{(N)} = 1 - \frac{(I_N - I_{max})}{(I_0 - I_{max})} \quad (2)$$

Where I_N is the cumulative brightness of the image at speed, N, I_0 represents the image brightness when the system is stationary and fully settled and I_{max} denotes when the system is completely suspended. Conditions of full suspension were associated to $S_{(N)} = 95$ %.

2.4. Culture of iPSCs and Characterization

2.4.1. iPSC Expansion and Cardiomyocyte Differentiation

Cell culture experiments were carried out using two bioreactor configurations (see Section 2.2). The iPSC expansion and differentiation protocols previously reported by Correia *et al.* (2014) were followed. Briefly, a murine transgenic αPIG-iPS cell line, kindly provided by Dr Tomo Saric (University of Cologne), was used where the puromycin-N-acetyl transferase gene was under the control of the cardiac-specific promotor, alpha-myosin heavy chain (α-MHC). iPSCs were expanded in static adherent monolayer cultures on inactivated murine embryonic fibroblasts (iMEFs) in expansion culture medium: Dulbecco's modified Eagle medium, (DMEM + GlutaMAX + 4.5 g/L D-Glucose), supplemented with 15 % (v/v) fetal bovine serum (FBS), 1 % (v/v) non-essential amino acids (NEAA), 2 mM L- glutamine, 50 μM β-mercaptoethanol, 500 μg/mL neomycin sulfate (all from Thermo Fisher Scientific, USA), and 1000 U/mL leukemia inhibitory factor (LIF) (ESGRO, Merck Millipore, Germany) maintained at 37 °C in a humidified atmosphere of 5 % (v/v) CO_2. Cultures were passaged every two days according to the protocol used by Correia *et al.* (2014). For bioreactor experiments, iPSCs were used at low passage numbers (between passage 6 and 8).

To initiate cardiogenic differentiation, iPSCs were aggregated to form embryoid bodies (EBs) in orbitally shaken Erlenmeyer flasks (Corning, USA) agitated at N = 80 rpm (day 0). Cells were inoculated at 0.7×10^5 cells/mL in V_w = 100 mL of differentiation medium comprising of Iscove's modified Dulbecco's medium (IMDM + GlutaMAX) supplemented with 20 % (v/v) FBS, 1 × NEAA, 1 % (v/v) Pen/Strep, 50 μM β-mercaptoethanol (all from Thermo Fisher

Scientific, USA) and 100 μM ascorbic acid (Wako, Germany), incubated at 37 °C in a humidified atmosphere of 5 % (v/v) CO_2. On day 1, shaking frequency was increased to N = 90 rpm. On day 2 aggregates were transferred to the bioreactors at a concentration of 150 aggregates/mL, using a total volume V_w = 200 mL of differentiation media. Cultures were run until day 9 under controlled dissolved oxygen (DO) and temperature (T) conditions [CO_2: 5 %; DO: 4 % O_2 Tension; Aeration: 0.1 VVM; T: 37 °C] whilst pH was monitored. For each experimental run, one magnetic and one motor-driven agitation culture were performed in parallel. The magnetically-driven control condition was operated at N = 90 rpm, T_{inv} = 30 s and T_{dwell} = 900 ms according to the most favorable differentiation yield condition, previously reported by Correia *et al.* (2014). Motor-driven agitation was performed at N = 90 rpm, T_{inv} = 30 s for two experimental runs at T_{dwell} = 500 ms and 1500 ms. Samples were withdrawn at day 2, 4, 6, 7 and 9 for subsequent analysis.

2.4.2. Cell Culture Characterization

Aggregate concentration and morphology were assessed using an inverted microscope (DMI6000, Leica) of 1 mL samples, distributed into 10 wells of a 24 well plate. Image analysis using ImageJ open source software (National Institutes of Health, USA) captured aggregate diameter, roundness and elongation. For determination of cell concentration and viability, aggregates were dissociated using 0.25 % Trypsin-EDTA at 37 °C. Viable cell counts were performed using a Fuchs-Rosenthal hemocytometer following incubation of cells in Trypan Blue dye 0.1 % (v/v) in PBS (all reagents from Thermo Fisher Scientific, USA). Cell viability and membrane integrity were also evaluated through incubation of the cells with enzyme substrate fluorescein diacetate (FDA) and the DNA-dye propidium iodide (PI) (both Sigma-Aldrich, Germany). Metabolic activity of the cells was quantified through measurement of glucose and lactate concentration in spun-down sample supernatants using the YSI 7100 MBS system (YSI Life Sciences, USA). Phenotypic analysis of cell samples at

the start (day 0) and end of differentiation (day 9) were assessed using flow cytometry. Aggregate samples were again dissociated before labelling with a primary antibody or isotype control for 1 h at 4 °C. For pluripotency assessment on day 0, OCT-4 and SSEA-1 markers were used (all antibodies obtained from BD, USA). On day 9 cardiac specific marker cardiac troponin T (cTnT) was assessed (Thermo Fisher Scientific, USA). 10,000 events per sample were registered using a CyFlow® space instrument (Sysmex Partec GmbH, Germany).

Cardiomyocyte purity was determined by flow cytometry of cTnT-positive cells on day 9 of differentiation in the bioreactor. Cardiomyocyte number was estimated by multiplying Cardiomyocyte purity by the number of viable cells, also determined on day 9. Cardiomyocyte yield was calculated by the number of cTnT-positive cells divided by the initial number of iPSCs. More information on the protocols followed to assess the cell culture can be found in a number of publications (Abecasis et al., 2017; Correia et al., 2014; Serra et al., 2011).

3. Results and Discussion

3.1. Frequency Analysis and Impact of Time Components

The first part of this study aimed at characterizing the energy spectrum of the tangential velocity for the three agitation modes employed by Correia *et al*. (2014) to understand whether a correlation exists between these frequencies and the differentiation yield. Figure 2 shows the energy spectra, kinetic energy per unit of frequency ($E_\theta(f)$), obtained for both continuous and intermittent agitation (N = 90 rpm) close to the impeller (location **A** Figure 1). As expected, the energy spectrum obtained for continuous agitation shows two significant peaks at f = 1.5 and 3.0 Hz, resulting from the periodic rotation of the two-blade impeller, whilst the other lower intensity peaks are harmonics of the main two (Figure 2 A). The

energy spectrum for the intermittent agitation without a direction change (Figure 2 B) shows similar frequency peaks at f = 1.5 and 3.0 Hz, corresponding to the impeller blade passage, in addition to a lower range of frequency peaks, which are harmonics of the interval time frequency, $f_{inv} = 1/T_{inv}$ = 0.03 Hz. The CM differentiation yield obtained using this agitation mode was the maximum reported by Correia *et al.* (2014). The measurement point, **A**, is located near the impeller blades and so a secondary measurement position was selected, at location **B** of Figure 1, to determine whether the low frequency peaks were present in the bulk flow. This can be seen in Figure 3. It is interesting to note that the energy intensity of the low frequency peaks was less affected by the measurement locations (30 %) in comparison to the peak intensities associated to the blade passage, which were significantly reduced (> 90 %) at location **B**. It is therefore evident that intermittent agitation introduced low frequency flow structures at a reactor scale, which could have influenced the EB suspension during differentiation. Figure 2 (C) shows the energy spectrum obtained when intermittent agitation with a direction change was implemented. The low frequency peaks (harmonics of $1/T_{inv}$) are also present in this case, however the addition of a direction change resulted in 1000-fold amplification of the energy associated with these frequencies. The CM differentiation yield achieved using this agitation mode was the lowest tested by Correia *et al.* (2014). These initial findings suggest that the low frequency peaks resulting from the use of intermittent agitation may have had a beneficial impact upon differentiation yield, spectrum of Figure 2 (B), however a maximum limit of energy density associated to these frequencies might exist, spectrum of Figure 2 (C), beyond which the low frequency flow structures associated to intermittent agitation becomes detrimental to the differentiation process.

The subsequent part of the study explored how each time component would impact upon the characteristic flow frequencies present. Figure 4 shows the energy spectra obtained at location **A** for N = 90 rpm when intermittent agitation parameters, T_{inv} and T_{dwell}, were varied.

Figure 4 (A) – (C) show the resultant energy spectra at decreasing interval times of T_{inv} = 30, 15 and 5 s, respectively (N = 90 rpm and T_{dwell} = 500 ms). As previously observed, the spectra show the low frequency peaks, in addition to the standard peaks corresponding to impeller blade passage. When T_{inv} is decreased the low frequency peaks are spread over a larger frequency range, and their intensity is amplified (see insets). Figure 4 (D) – (F) show the energy spectra for increasing dwell time at T_{dwell} = 500, 1000 and 1500 ms, respectively (N = 90 rpm and T_{inv} = 30 s). In this case the frequency range is not affected, but as T_{dwell} increases from 500 ms (D) to 1500 ms (F) (see insets), the low frequency peaks increase in intensity. To better quantify the energy density variation with T_{dwell}, Figure 5 shows the integral of the energy associated with the low frequency peaks for T_{dwell} = 1 – 1500 ms at N = 90 rpm and T_{inv} = 30 s. The corresponding cumulative energy increases significantly with an increase in the number of missed revolutions (i.e. $N \times T_{dwell}$).

Once the impact of the individual time components (N, T_{dwell} and T_{inv}) had been investigated, it was attempted to determine a scale-invariant parameter at which the low frequency peaks would be the same for different operating conditions. From this point of view, the possibility to recreate the low frequency peaks originally implemented in the work of Correia with an alternative selection of operating conditions (N, T_{dwell} and T_{inv}), could establish a more robust procedure for cell differentiation. The number of missed revolutions, K^{**}, defined in Equation (1), was the selected parameter to be kept constant. Experiments were conducted at different rotational speeds in the range of 75 – 120 rpm, where K^{**}= 2.25. The resultant spectra are shown in Figure 6 (A – D). As it can be observed from the insets, all experiments exhibited similar low frequency peaks when K^{**} was kept constant. It is therefore evident that the number of missed revolutions can be effectively used as a decisional and scalable parameter to consistently recreate a low frequency spectrum, promoting differentiating yields.

As a proof of concept, the study reported in Section 3.2, was therefore designed to further assess how variation of the low frequency peaks characteristics, induced by variation of K^{**} and T_{dwell}, affect cell differentiation.

3.2. Impact of T_{dwell} on Cardiogenic iPSC Differentiation

The second stage of our study sought to obtain biological verification of the impact of T_{dwell} on CM differentiation yield, based on the hypothesis that the presence of low frequency peaks influences cardiogenic differentiation. The previous section highlighted that two main flow parameters were affected through variation of the three time components; the spectrum peak intensities and the associated frequencies. As shown in Section 3.1, Figure 4, adjustment of T_{dwell} singularly affected the energy intensity associated to the low frequency peaks. Adjustment of T_{inv} not only impacted upon energy intensity, but also upon the range of low frequency peaks generated. To singularly investigate the impact with changing the peak frequencies at a constant energy intensity, both T_{inv} and T_{dwell} would need to be simultaneously adjusted. The published CM differentiation yields of (Correia et al., 2014) showed the best and worst performing agitation modes were associated to the lowest and highest, respectively, peak intensities for the low frequency region. For an initial proof of concept investigation, given the complexity of the biological system, modulation of a single time component, T_{dwell}, was selected to observe the biological outcomes associated to the singular change of peak intensities in the energy spectra obtained.

Two experiments were conducted from monoloayer iPSC expansion to EB formation before inoculation in bioreactors, where two discrete intermittent agitation modes were employed, both in parallel to a control condition. The control condition utilized magnetically-driven intermittent agitation without a direction change.

Phenotypic analysis at day 0 of each experimental run indicated a largely pluripotent cell population expressing OCT-4 and SSEA-1 at 87.35 ± 3.7 % and 86.11 ± 1.7 %, respectively (data not shown). All bioreactors were inoculated at day 2 and showed relative uniformity in aggregate size, D_{50} = 164.43 ± 14.54 μm and concentration, 159 ± 5 aggregates/mL. Cells remained largely viable over the course of differentiation, as shown by cell aggregate FDA/PI live stains at the end of differentiation in Figure 7 (A), with Figure 7 (B) showing aggregate size and morphology determined through cell images, both on day 9. As indicated in Figure 7 (B), large variability in aggregate size was observed in all conditions, with D_{50} = 221.7 ± 141.7 μm, 195.3 ± 128 μm and 190 ± 172 μm for the control condition, T_{dwell} = 500 ms and T_{dwell} = 1500 ms, respectively. Overall, an approximate 25 % increase in D_{50} was observed from day 2 to day 9 in all conditions. Measurements of aggregate roundness demonstrated that no significant differences can be noted between the experimental conditions tested. Cell phenotype was assessed at the end of differentiation for the cardiomyocyte-specific marker, cTnT using flow cytometry. This was used as a measure of CM purity and to determine the overall differentiation yield. Table I summarizes these results for each experimental condition, comparing cardiomyocyte purity, number and overall yield (measured as the number of CMs/input iPSC) obtained using two motor-driven agitation conditions, T_{dwell} = 500 ms and T_{dwell} = 1500 ms, each normalized against the control condition for each run. Results show that as T_{dwell} is increased from 500 ms cardiomyocyte differentiation efficiency increases (Error! Reference source not found.). In particular, CM number and yield increased by 1.27 and 1.66 – fold (+ 27 % and + 66 %), respectively, at T_{dwell} = 1500 ms when compared to the control condition at T_{dwell} = 900 ms. Concordantly, CM number and yield decreased for T_{dwell} = 500 ms when compared to the control at T_{dwell} = 900 ms by 0.85 and 0.8 – fold (- 15 % and – 20 %), respectively. Overall, Table I shows no significant differences in CM purity between different experimental runs. Purity was not compromised throughout the

biological cultures as the differences observed for purity were within the experimental error, as given in Table I. The literature suggests the addition of mechanical cues has an impact upon CM differentiation, cell growth and morphology (Geuss and Suggs, 2013; Savla et al., 2014). The differences observed between CM number and CM yield (Table I) are due to the variability in the inoculum iPSC density, since aggregate concentration at inoculation is the parameter that was maintained constant between runs, as was done previously (Correia et al 2014). Thus, we have presented both values to show that adjustment of T_{dwell} impacts upon CM differentiation efficiency mostly through CM number and yield instead of CM purity (Error! Reference source not found.). This was not related to the generation of aggregates with significant changes in average size and morphology (Figure 7), which were found to be very similar among all conditions.

This initial proof of concept study has shown that a conservative 10-fold amplification of the low frequency peaks, from T_{dwell} = 900 ms to 1500 ms, is beneficial for cardiomyocyte differentiation of iPSCs through improved generation of high numbers of cardiomyocytes. The experimental findings for intermittent agitation with a direction change, reported by Correia *et al.*, showed the detrimental impact of significant (1000-fold) amplification of the low frequency peaks (Figure 2 C) to CM differentiation yields. What becomes evident is a threshold limit for low frequency peak amplification which accentuates that careful selection of operating conditions is paramount when considering a cell culture in its entirety.

3.3. Embryoid Body Suspension Characterization

In the literature cell culture studies often lack rigorous suspension characterization in bioreactors. The final part of this study sought to first determine the minimum speeds required to reach complete suspension and system homogeneity under continuous agitation for Cytodex 3 ($EB_{(start)}$) and for Cultispher-G ($EB_{(end)}$). These were found to be $N_{H[start]}$ = 39

rpm and $N_{H[end]}$ = 52 rpm, confirming that at our selected speed, N = 90 rpm, full homogeneity throughout the culture time is achieved. Suspension during intermittent agitation conditions was also investigated. The EB suspension index, S, obtained using the two EB mimics ($EB_{(start)}$ and $EB_{(end)}$) for N = 90 rpm, T_{inv} = 30 s and T_{dwell} = 30,000 ms, is represented in Figure 8 (A) and (B), respectively. Figure 8 (A) shows a maximum 20 % drop in suspension is attained during the dwell time for $EB_{(start)}$, which significantly increases to a 65 % drop at the end of differentiation ($EB_{(end)}$) (Figure 8 B). This suggests the extent of settling may have a more significant influence on the process performance, especially at the end of the differentiation process where the EBs increase in size. As discussed in Section 3.1, the main frequency peaks corresponding to impeller blade passage are associated with higher energy in areas close to the impeller region. In Figure 8 (B) the EBs occupy the bottom 35% of the tank around the impeller during the dwell. Upon resuspension they will be exposed to the higher energy introduced by impeller blade rotation. T_{dwell} could be adjusted towards the end of differentiation to maintain the optimal level of suspension throughout the culture time and to avoid accumulation around the impeller and, consequently, exposure to higher energy. To determine the extent of settling during the dwell time, the minima of the suspension that occurred is shown in Figure 9. For the validation cell culture experiments T_{dwell} = 500, 900 and 1500 ms were investigated. Interestingly, Figure 9 shows suspension to drop less than 1 % across these conditions. It can be observed that as T_{dwell} increases, the maximal extent of settling increases, an effect which becomes more pronounced for $EB_{(end)}$. In the same graph, the time needed to resuspend, $t_{resuspend}$, for each EB mimic is also plotted. Upon restarting of the impeller motion, resuspension of the EBs occurs rapidly, taking between 2 and 4 s to become fully suspended. The data of Figure 9 shows that the level of settling, especially at the end of the process, must be carefully considered, while resuspension occurs rapidly and should not have a significant impact on the process. From this point of view Figure 9 can

instruct on the development of novel strategies to select and optimize the operating conditions for biological processes.

4. Conclusions

These studies have supported the establishment of a relationship between the hydrodynamic environment and the biological outcomes associated with the engineering characteristics. It is evident that an optimal range of characteristic frequencies exists, and a combination of engineering and biological experimental approaches is essential to improve current knowledge and exploit mechanical cues to optimize cell differentiation processes. Initial proof of concept biological studies have shown that a conservative 10-fold amplification of the characteristic low frequency peaks resulted in a more optimal hydrodynamic environment for cardiogenic differentiation. 1000-fold amplification in low frequency peaks achieved with intermittent agitation with a direction change, investigated previously, reduced CM differentiation efficiency. This suggests the existence of an optimum threshold of the energy contained in the low frequency peaks. Further studies investigating the impact of the remaining two time components, N and T_{inv}, on biological behaviour are needed. The impact of intermittent motion on mixing characteristics and shear effects must also be characterized to further understand how each engineering parameter correlates to biological behavioral outcomes. Enhancing CM yields increases the cost-effectiveness of CMs produced/liter. This in turn would then contribute to the development of mass, therapeutic production of CMs, through modulation of the microenvironment alone. This would reduce the need for additional chemical factors or longer differentiation protocols. This work provides a proof of concept biological study to identify the engineering aspects most affecting the differentiation process. The proof of concept was based on a well-established differentiation platform (a murine iPSC cell line with a spontaneous differentiation protocol), which has already been published in the literature (see Correia *et al.* (2014)). Successive works can validate the

outcomes discussed herein and transfer the knowledge obtained to an optimized directed differentiation protocol with more clinically relevant human PSC lines.

5. Acknowledgments

We thank Dr Paula M. Alves and Dr António Roldão for fruitful discussions. We also acknowledge Eng. Marcos Sousa for technical support on cell culture experiments. This work was supported by the Centre for Doctoral Training (CDT) in Innovative Manufacturing in Emerging Macromolecular Therapies, EPSRC [EP/L015218/1], by the European Union's Horizon 2020 research and innovation programme [grant agreement No: 739572], by the Fundação para a Ciência e Tecnologia (FCT)-funded project CARDIOSTEM [MITPTB/ECE/0013/2013] and iNOVA4Health Research Unit [LISBOA-01-0145-FEDER-007344], which is cofunded by FCT/MCES, through national funds, and by FEDER under the PT2020 Partnership Agreement.

References

Abecasis, B., Aguiar, T., Arnault, É., Costa, R., Gomes-Alves, P., Aspegren, A., Serra, M., Alves, P.M., 2017. Expansion of 3D human induced pluripotent stem cell aggregates in bioreactors: Bioprocess intensification and scaling-up approaches. J. Biotechnol. 246, 81–93. https://doi.org/10.1016/j.jbiotec.2017.01.004

Correia, C., Serra, M., Espinha, N., Sousa, M., Brito, C., Burkert, K., Zheng, Y., Hescheler, J., Carrondo, M.J.T., Sarić, T., Alves, P.M., 2014. Combining hypoxia and bioreactor hydrodynamics boosts induced pluripotent stem cell differentiation towards cardiomyocytes. Stem Cell Rev. 10, 786–801. https://doi.org/10.1007/s12015-014-9533-0

Ge, D., Liu, X., Li, L., Wu, J., Tu, Q., Shi, Y., Chen, H., 2009. Chemical and physical stimuli induce cardiomyocyte differentiation from stem cells. Biochem. Biophys. Res.

Commun. 381, 317–321. https://doi.org/10.1016/j.bbrc.2009.01.173

Geuss, L.R., Suggs, L.J., 2013. Making cardiomyocytes: how mechanical stimulation can influence differentiation of pluripotent stem cells. Biotechnol. Prog. 29, 1089–96. https://doi.org/10.1002/btpr.1794

Ibrahim, S., Nienow, A.W., 2004. Suspension of microcarriers for cell culture with axial flow impellers. Chem. Eng. Res. Des. 82, 1082–1088. https://doi.org/10.1205/cerd.82.9.1082.44161

Kehat, I., Kenyagin-Karsenti, D., Snir, M., Segev, H., Amit, M., Gepstein, A., Livne, E., Binah, O., Itskovitz-Eldor, J., Gepstein, L., 2001. Human embryonic stem cells can differentiate into myocytes with structural and functional properties of cardiomyocytes. J Clin Invest 108, 407–414. https://doi.org/10.1172/JCI12131

Lam, A.T.-L., Chen, A.K.-L., Li, J., Birch, W.R., Reuveny, S., Oh, S.K.-W., 2014. Conjoint propagation and differentiation of human embryonic stem cells to cardiomyocytes in a defined microcarrier spinner culture. Stem Cell Res. Ther. 5, 110. https://doi.org/10.1186/scrt498

Lara, A.R., Galindo, E., Ramírez, O.T., Palomares, L.A., 2006. Living with heterogeneities in bioreactors: understanding the effects of environmental gradients on cells. Mol. Biotechnol. 34, 355–382. https://doi.org/10.1385/MB:34:3:355

Nienow, A.W., Coopman, K., Heathman, T.R.J., Rafiq, Q.A., Hewitt, C.J., 2016. Bioreactor Engineering Fundamentals for Stem Cell Manufacturing, in: Stem Cell Manufacturing. pp. 43–75. https://doi.org/10.1016/B978-0-444-63265-4.00003-0

Olmos, E., Loubiere, K., Martin, C., Delaplace, G., Marc, A., 2015. Critical agitation for microcarrier suspension in orbital shaken bioreactors: Experimental study and

dimensional analysis. Chem. Eng. Sci. 122, 545–554. https://doi.org/10.1016/j.ces.2014.08.063

Pieralisi, I., Rodriguez, G., Micheletti, M., Paglianti, A., Ducci, A., 2016. Microcarriers' suspension and flow dynamics in orbitally shaken bioreactors. Chem. Eng. Res. Des. 108, 198–209. https://doi.org/10.1016/j.cherd.2015.11.020

Savla, J.J., Nelson, B.C., Perry, C.N., Adler, E.D., 2014. Induced pluripotent stem cells for the study of cardiovascular disease. J. Am. Coll. Cardiol. 64, 512–9. https://doi.org/10.1016/j.jacc.2014.05.038

Serra, M., Correia, C., Malpique, R., Brito, C., Jensen, J., Bjorquist, P., Carrondo, M.J.T., Alves, P.M., 2011. Microencapsulation technology: a powerful tool for integrating expansion and cryopreservation of human embryonic stem cells. PLoS One 6, e23212. https://doi.org/10.1371/journal.pone.0023212

Ting, S., Chen, A., Reuveny, S., Oh, S., 2014. An intermittent rocking platform for integrated expansion and differentiation of human pluripotent stem cells to cardiomyocytes in suspended microcarrier cultures. Stem Cell Res. 13, 202–13. https://doi.org/10.1016/j.scr.2014.06.002

	T_{dwell} **500**	T_{dwell} **1500**
Cardiomyocyte Purity [% cTnT positive*]	1.11 ± 0.23	0.95 ± 0.20
Cardiomyocyte Number [-]	0.85 ± 0.03	1.27 ± 0.04
Cardiomyocyte Yield [#CMs/input iPSC]	0.80 ± 0.06	1.66 ± 0.12

Table I: Cardiomyocyte number, yield and purity determined on day 9 of differentiation in stirred tank bioreactors operated under intermittent agitation with a T_{dwell} of 500ms (T_{dwell} 500) and 1500ms (T_{dwell} 1500). Results were shown as fold change when compared to the magnetic agitation control condition (T_{dwell} of 900ms) run in parallel.

Figure 1: Schematic diagram of the experimental setup. A and B indicate two laser measurement locations.

Figure 2: Energy spectra of the instantaneous tangential velocity. (A) Continuous agitation [N = 90 rpm]. (B) Intermittent agitation without direction change [N = 90 rpm, T_{inv} = 30 s, T_{dwell} = 900 ms]. (C) Intermittent agitation with direction change [N = 90 rpm, T_{inv} = 30 s].

Figure 3: Energy spectra of the instantaneous tangential velocity data at intermittent agitation motion. (A) Measurement location **A**, [N = 90 rpm, T_{inv} = 30 s, T_{dwell} = 500 ms]. (B) Measurement location **B**, [N = 90 rpm, T_{inv} = 30 s, T_{dwell} = 500 ms].

Figure 4: Energy spectra of the instantaneous tangential velocity data at intermittent agitation motion. (A) – (C): N = 90 rpm, T_{inv} = 30 s, 15 s, 5 s, T_{dwell} = 500 ms. (D) – (F): N = 90 rpm, T_{inv} = 30 s, T_{dwell} = 500 ms, 1000 ms, 1500 ms.

Figure 5: Low frequency kinetic energy summation with increasing T_{dwell}.

Figure 6: Energy spectra of the instantaneous tangential velocity data at intermittent impeller motion and at constant $K^{**} = 2.25$. (A): N = 75 rpm, T_{inv} = 30 s, T_{dwell} = 1800 ms. (B): N = 90 rpm, T_{inv} = 30 s, T_{dwell} = 1500 ms. (C): N = 105 rpm, T_{inv} = 30 s, T_{dwell} = 1290 ms. (D): N = 120 rpm, T_{inv} = 30 s, T_{dwell} = 1125 ms.

Figure 7: Day 9 iPSC-CM differentiation culture. (A) Live/dead cell stain of iPSC and cardiosphere aggregates from merged phase contrast and fluorescence images. (B) Measurement of aggregate characteristics: size and roundness.

Figure 8: Suspension characterisation of intermittent agitation over time [N = 90 rpm, T_{inv} = 30 s and T_{dwell} = 30 s]. (A) $EB_{(start)}$ [Cytodex 3]. (B) $EB_{(end)}$ [Cultispher-G].

Figure 9: Average drop in suspension and time to fully resuspend at increasing T_{dwell} [N = 90 rpm, T_{inv} = 30 s].

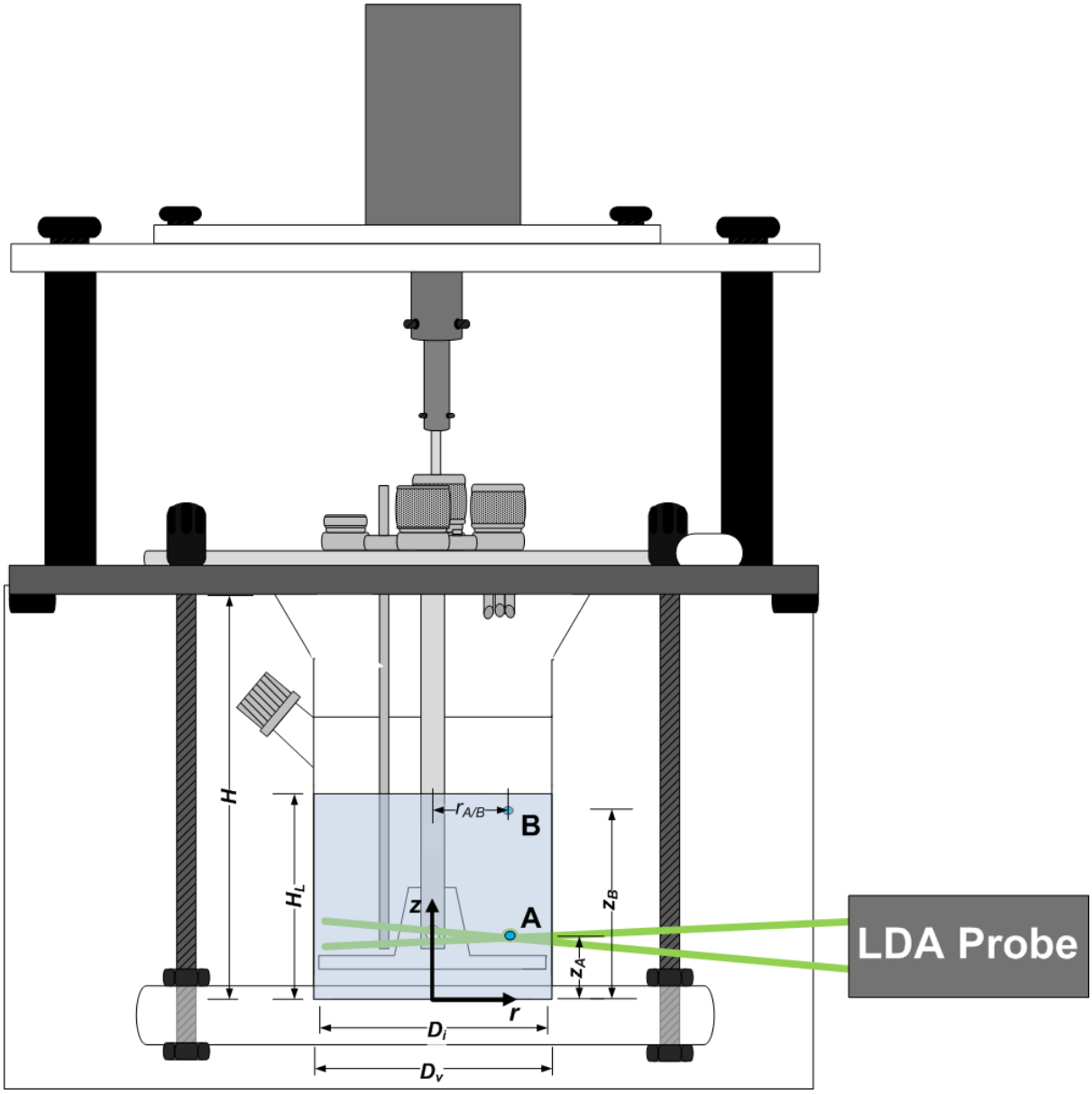

Figure 1

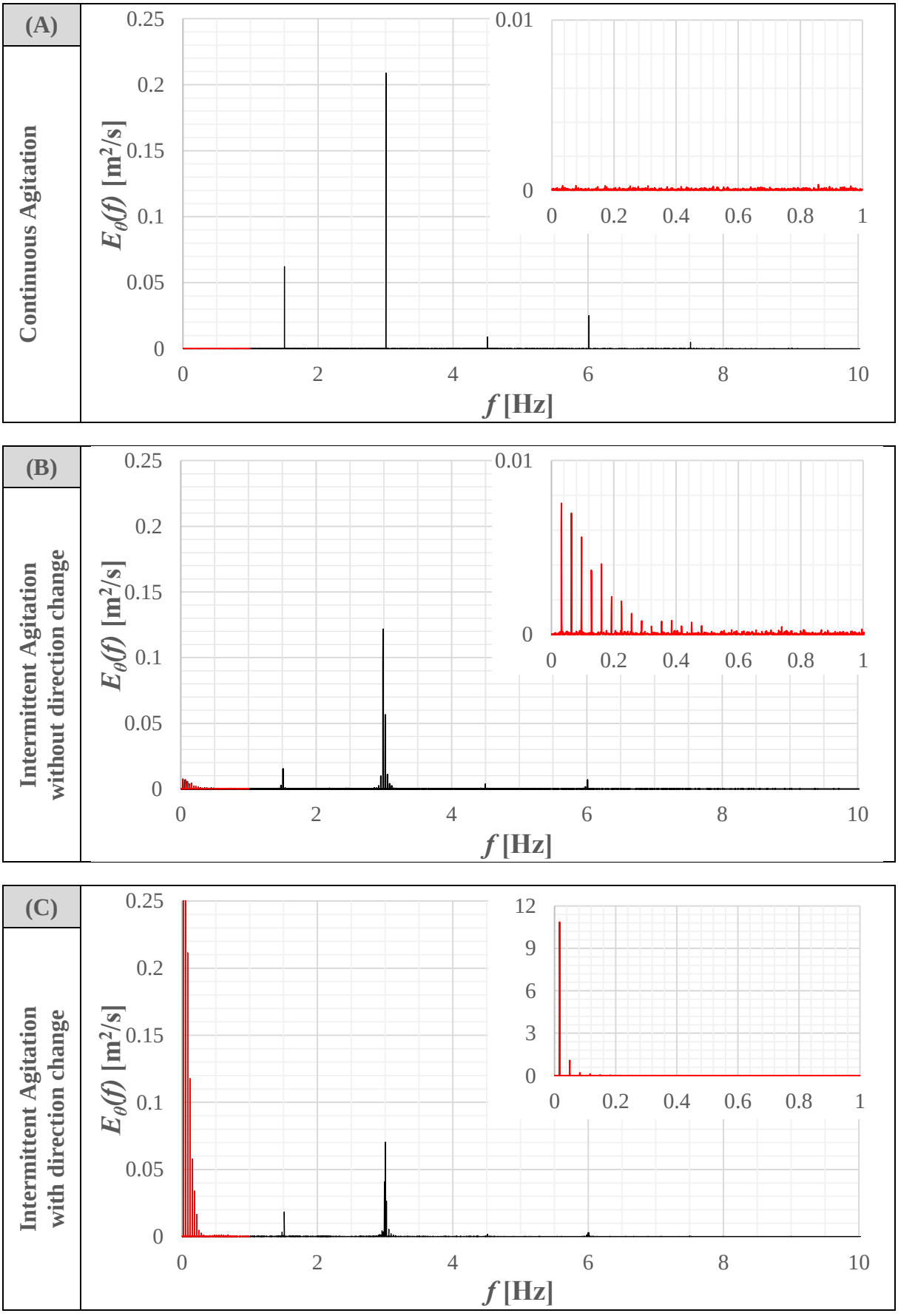
(A)
Continuous Agitation
(B)
Intermittent Agitation without direction change
(C)
Intermittent Agitation with direction change
$E_\theta(f)$ [m²/s]
f [Hz]
0.25
0.2
0.15
0.1
0.05
0
0.01
12
9
6
3
0
2
4
6
8
10
0.2
0.4
0.6
0.8
1

Figure 2

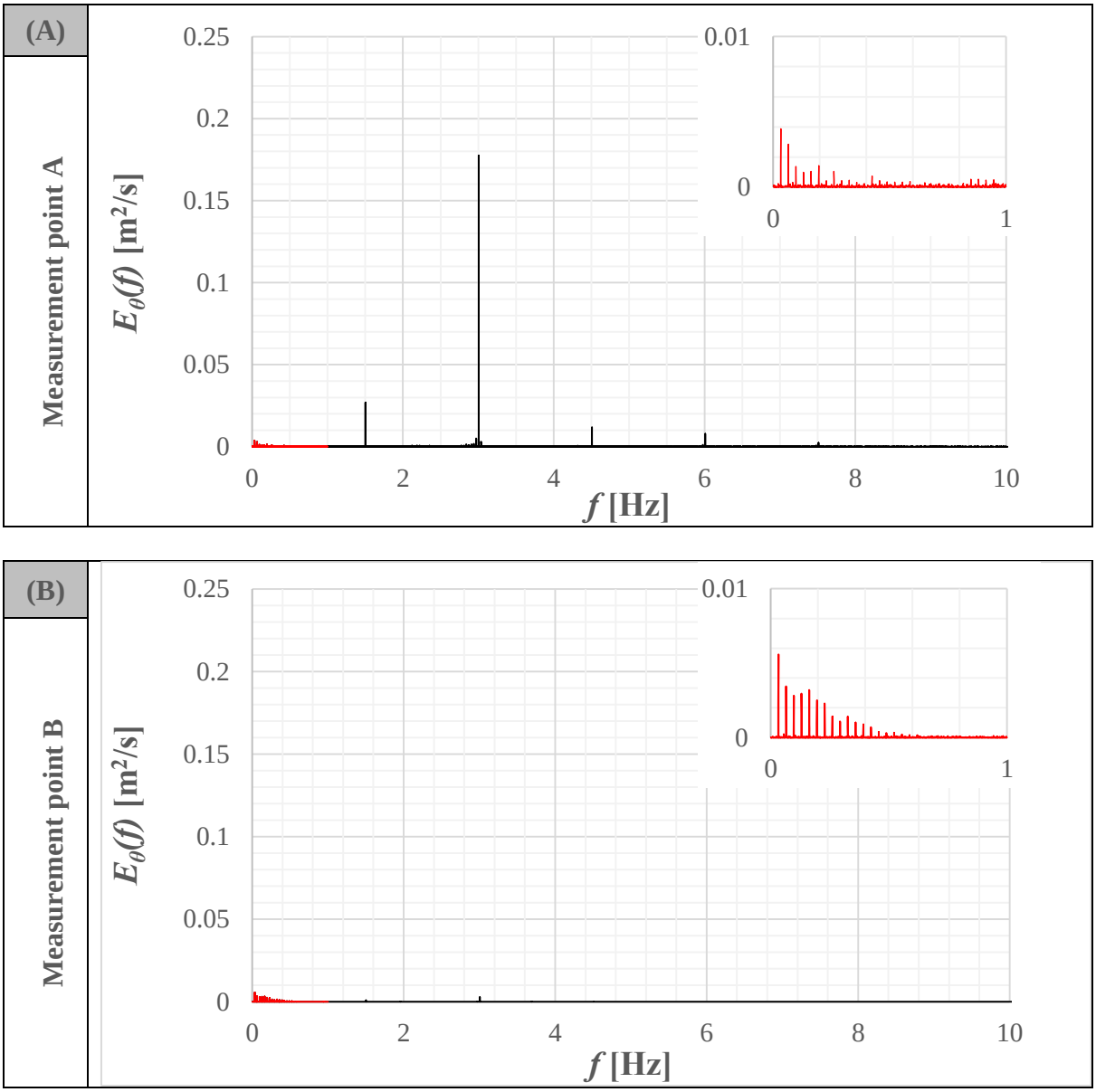
(A)
Measurement point A
$E_\theta(f)$ [m²/s]
0.25
0.2
0.15
0.1
0.05
0
0.01
0
0
1
0
2
4
6
8
10
f [Hz]
(B)
Measurement point B
$E_\theta(f)$ [m²/s]
0.25
0.2
0.15
0.1
0.05
0
0.01
0
0
1
0
2
4
6
8
10
f [Hz]

Figure 3

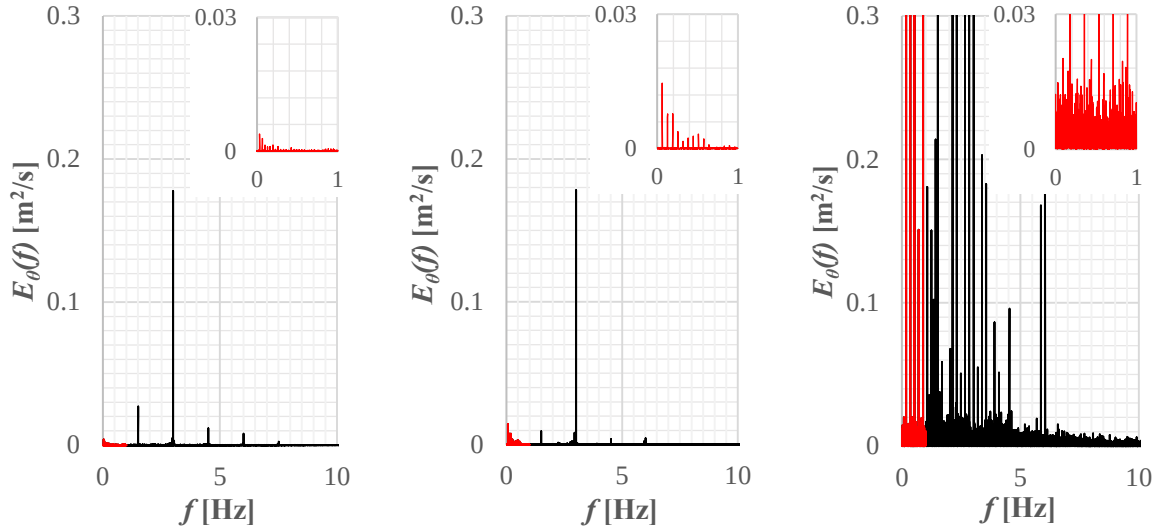

T_{inv} = 30 s (A)

T_{inv} = 15 s (B)

T_{inv} = 5 s (C)

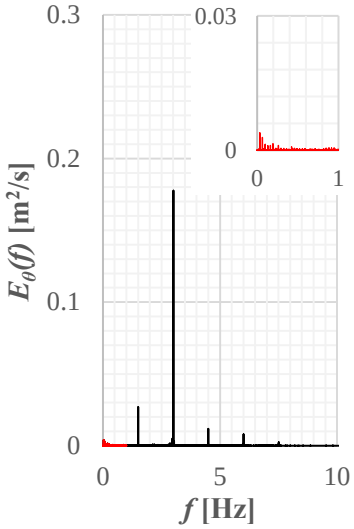

T_{dwell} = 500 ms (D)

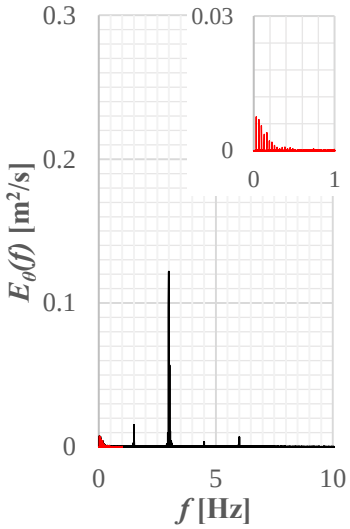

T_{dwell} = 1000 ms (E)

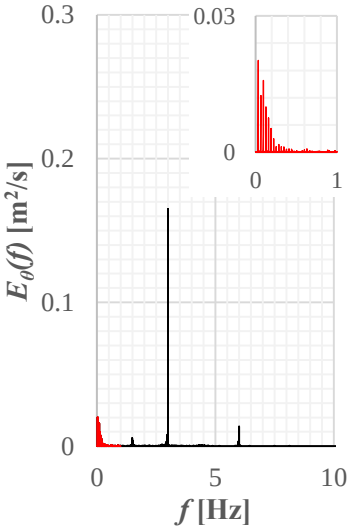

T_{dwell} = 1500 ms (F)

Figure 4

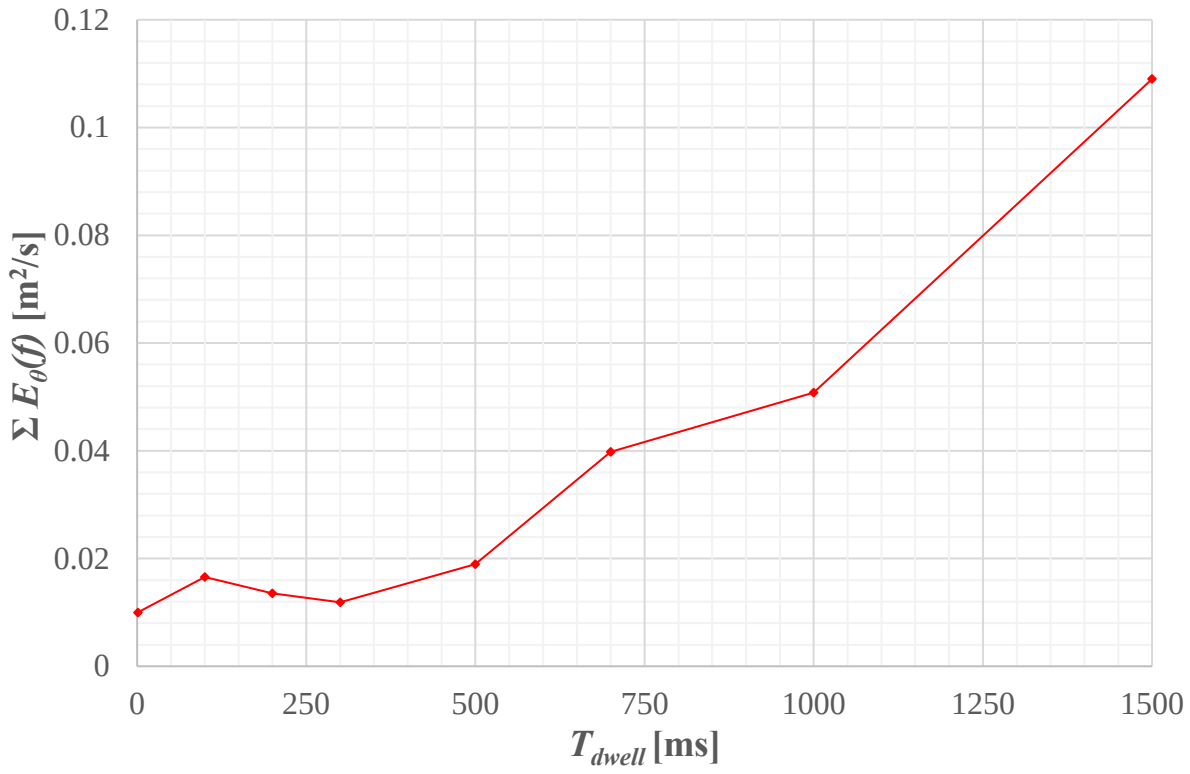
0.12
0.1
0.08
0.06
0.04
0.02
0
$\Sigma E_\theta(f)$ [m²/s]
0
250
500
750
1000
1250
1500
T_{dwell} [ms]

Figure 5

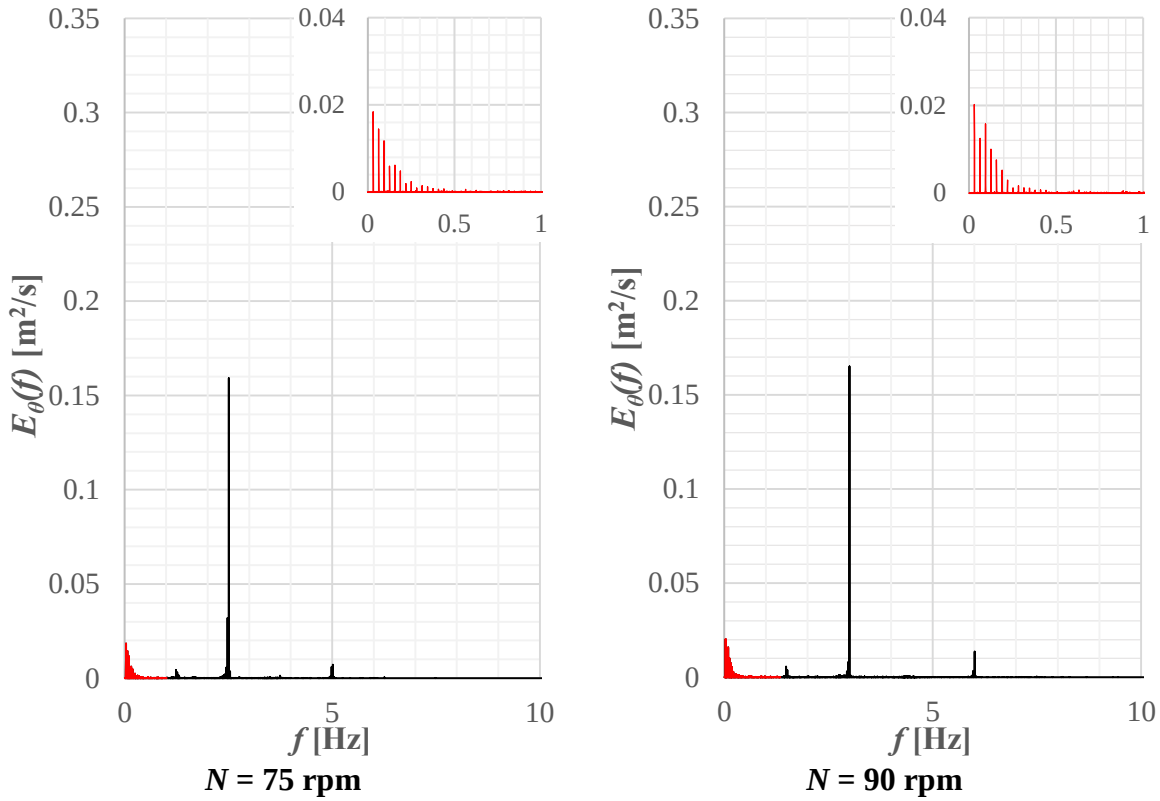

(A) (B)

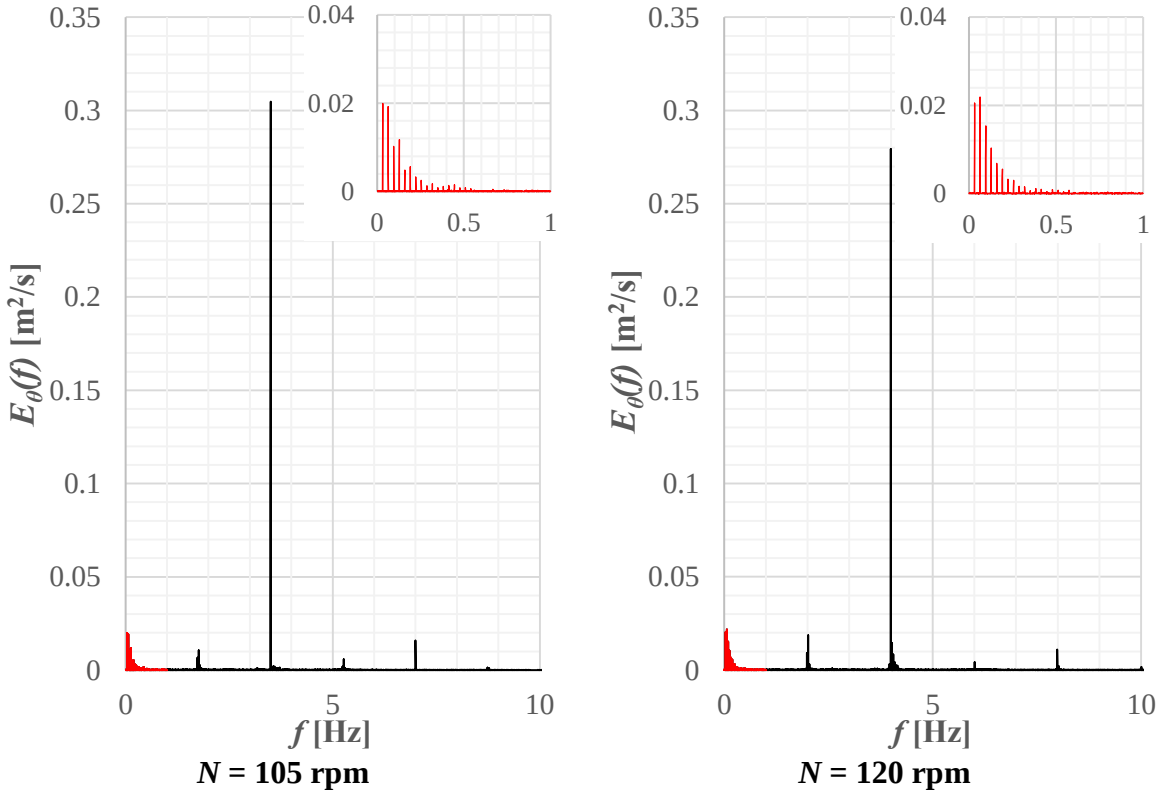

(C) (D)

Figure 6

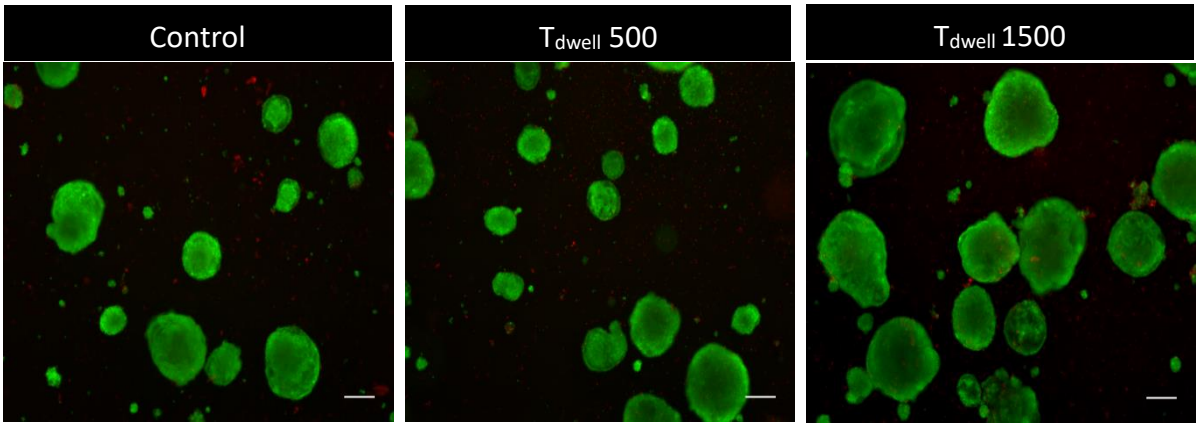
Control
Tdwell 500
Tdwell 1500

(A)

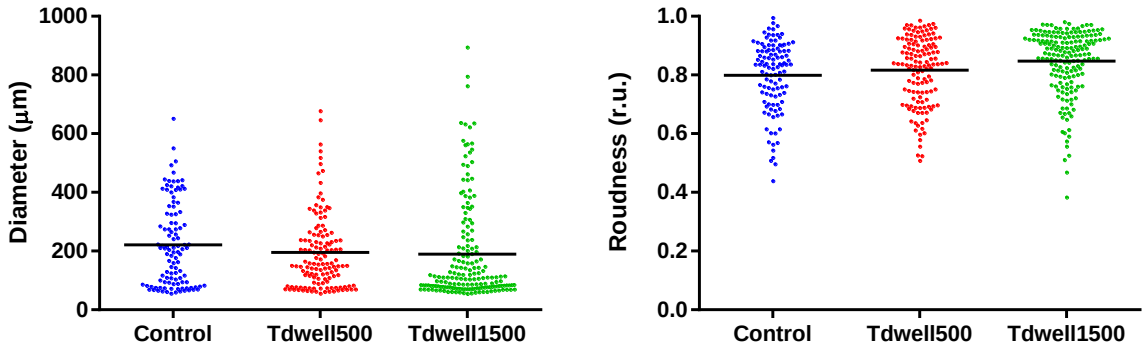
Diameter (µm)
1000
800
600
400
200
0
Control
Tdwell500
Tdwell1500
Roudness (r.u.)
1.0
0.8
0.6
0.4
0.2
0.0
Control
Tdwell500
Tdwell1500

(B)

Figure 7

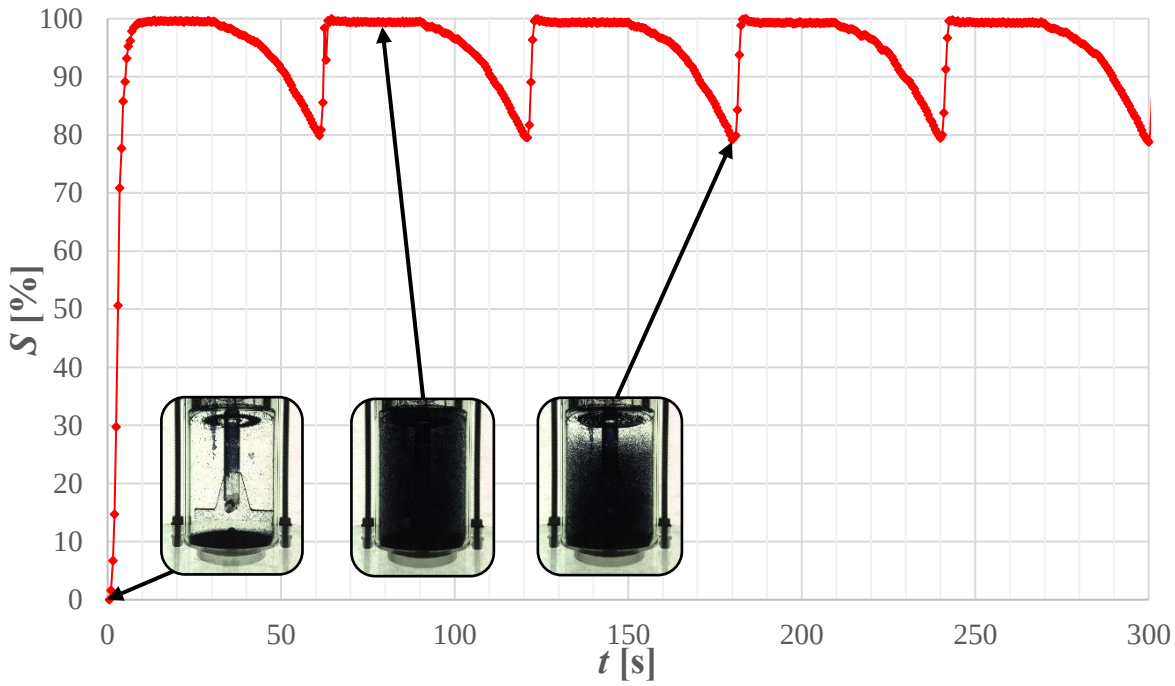
100
90
80
70
60
50
40
30
20
10
0
S [%]
0
50
100
150
200
250
300
t [s]

(A)

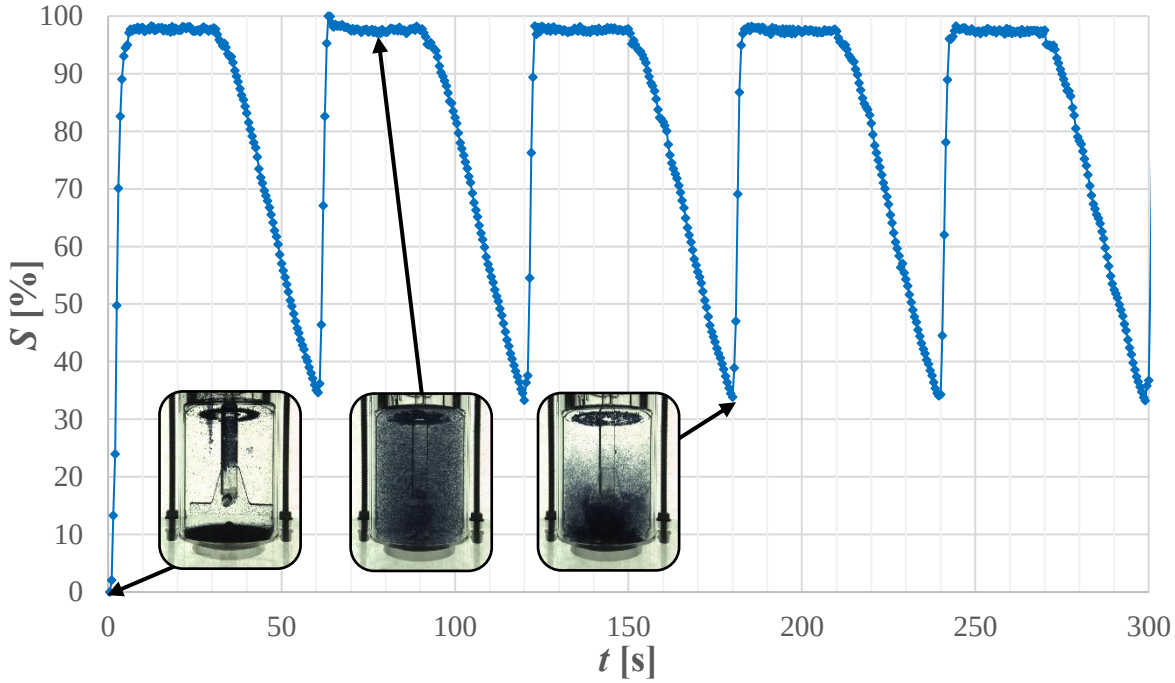
100
90
80
70
60
50
40
30
20
10
0
S [%]
0
50
100
150
200
250
300
t [s]

(B)

Figure 8

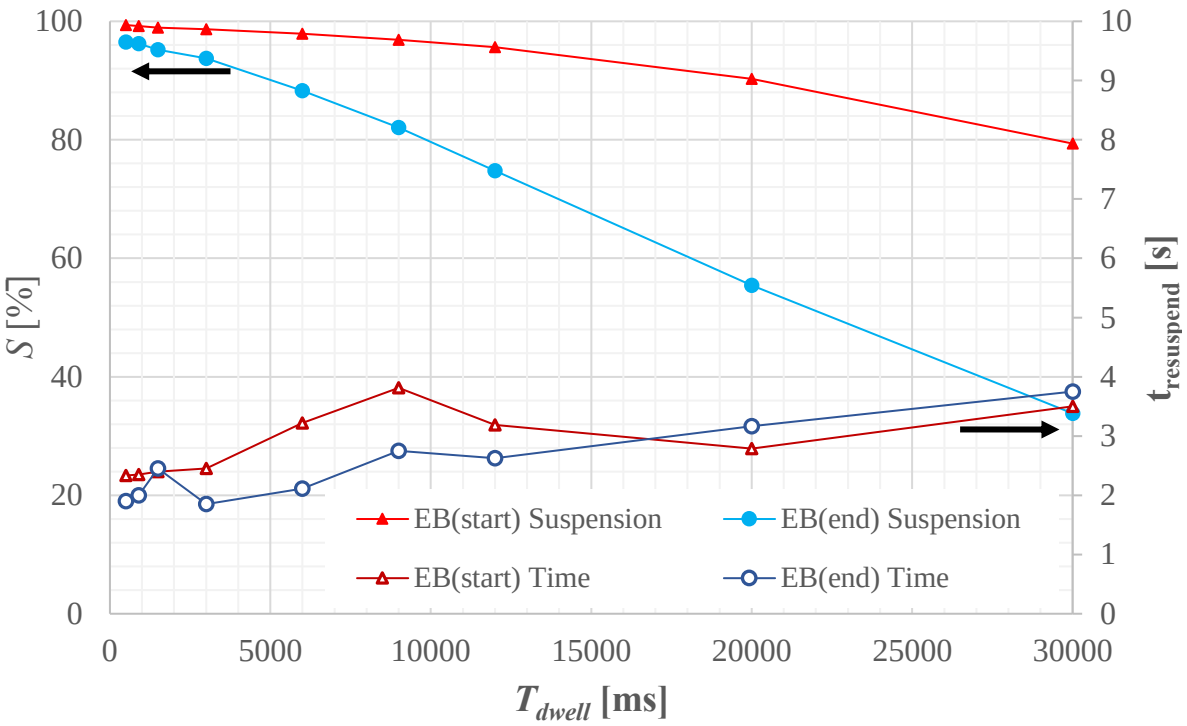
100
80
60
40
20
0
S [%]
10
9
8
7
6
5
4
3
2
1
0
t resuspend [s]
0
5000
10000
15000
20000
25000
30000
T dwell [ms]
EB(start) Suspension
EB(end) Suspension
EB(start) Time
EB(end) Time

Figure 9